Chapter 14
Examining Material Response Using X-Ray Phase Contrast Imaging

B. J. Jensen, B. Branch, F. J. Cherne, A. Mandal, D. S. Montgomery, A. J. Iverson, and C. Carlson

Abstract Propagation based X-ray phase contrast imaging (PCI) offers unique opportunities for ultrafast, high-resolution measurements to examine dynamic materials response at extreme conditions. Within the past decade, efforts on the IMPULSE system at the Advanced Photon Source included the development of a novel Multi-frame X-ray PCI (MPCI) system that was used to obtain the first shock-movies to examine material deformation with micron spatial resolution on nanosecond timescale. The MPCI system has been systematically developed over the years to improve optical efficiencies, spatial resolution, obtain more images per experiment, and to develop a dual-imaging, dual-zoom feature useful for many applications. With the MPCI system, X-ray PCI has been successfully used to study a wide range of phenomena including jet-formation in metals, crack nucleation and propagation, response of additively manufactured materials, and detonator dynamics to name a few. In this paper, a brief overview of the MPCI system development is provided along with its application to study shock propagation in materials.

Keywords PCI · phase contrast imaging · x-ray imaging · shock compression · matter at extremes

14.1 Introduction

Traditional shock wave experiments have proven successful over the years in relating the evolution of the shock wave propagation to the underlying mechanisms responsible for the material response [1–4]. Because these methods do not access the microscopic length scale directly, new diagnostics are needed that can provide real-time, in-situ, and spatially resolved measurements on the microscopic length scale with nanosecond time resolution. In recent years, there has been significant efforts in obtaining X-ray diffraction data in shock wave experiments [5–7] and in coupling dynamic loading platforms to the X-ray beam lines at Argonne National Laboratory's Advanced Photon Source (APS, Argonne, IL) to take advantage of diagnostics such as X-ray diffraction (XRD) and X-ray Phase Contrast Imaging (PCI) [8–11]. In particular, X-ray PCI provides a unique opportunity for acquiring high-resolution, spatially resolved, in-situ images of materials response and shock wave propagation during dynamic compression experiments. In the current work, X-ray PCI images of shock wave propagation through a polycarbonate sample were obtained to determine the in-situ shock wave velocity. The results were compared with the known shock response of the material and data obtained using traditional shock wave methods.

14.2 Experiments and Methods

Propagation based X-ray phase contrast imaging (PCI) is sensitive to differences in the index of refraction which is proportional to the density of the material. PCI requires a spatially coherent X-ray beam to achieve the enhanced contrast needed to bring out features within a material such as cracks, edges, and voids. The application to shock wave experiments was proposed by Montgomery [12] and first demonstrated experimentally at the Advanced Photon Source (APS; Argonne, IL) on the IMPULSE (**IMP**act System for **UL**trafast **S**ynchrotron **E**xperiments) gas gun system [8–11, 13]. Experiments on IMPULSE at the APS have been performed to study a wide range of phenomena including crack propagation in materials

B. J. Jensen (✉) · B. Branch · F. J. Cherne · A. Mandal · D. S. Montgomery
Los Alamos National Laboratory, Los Alamos, NM, USA
e-mail: bjjensen@lanl.gov

A. J. Iverson · C. Carlson
National Security Technologies, Los Alamos, NM, USA

J. Kimberley et al. (eds.), *Dynamic Behavior of Materials, Volume 1*, Conference Proceedings of the Society for Experimental Mechanics Series, https://doi.org/10.1007/978-3-319-95089-1_14

[14], jet formation in metals [15], dynamic extrusion tests on polymers [16, 17], response of additively manufactured (AM) materials to shock loading [18, 19], dynamic response of detonator initiator systems [20–22], compaction of powder materials [23], and response of explosives [24] to name a few.

The multi-frame X-ray PCI (MPCI) system in routine use at the APS and at the new Dynamic Compression Sector (DCS) consists of individually gated ICCD (Intensified charge coupled device) PI-MAX-4 cameras (Princeton Instruments, Inc.) optically multiplexed together to obtain sequential images (or "shock movies") during dynamic loading. A schematic of the system is shown in Fig. 14.1 and described in detail elsewhere [8–10, 15, 25, 26]. Briefly, X-rays from the synchrotron propagate through the sample and are incident upon a scintillator (typically LSO) which converts the X-rays to visible light. A series of optical components including mirrors (M1 and M2), beam splitters (BS), relay lenses (RL), and objective lenses (OB1 and OB2) image the light onto the ICCD cameras (ICCD 1–4). Because each ICCD is individually gated, the cameras can be synchronized with the desired X-ray bunch to capture a specific event during loading. Since its inception in 2011, the MPCI system has undergone significant improvement which includes the ability to take 8 images per experiment by interleaving in time four PI-MAX-4 ICCDs with the dual image feature (DIF). This feature allows for two images per camera with a minimum separation between images of at least 500 nanoseconds. The entire system is motorized for remote operation and optimization while the system is in the X-ray beam. Most recently, a dual imaging scheme for the scintillator (image both sides of the scintillator) has improved the light efficiency and allows the use of two different microscope objectives simultaneously (OB1 and OB2) for multiple magnification (5x, 7.5x, 10x) or fields-of-view (FOV) [21]. Note: to switch from the dual imaging mode (shown in Fig. 14.1) back to the standard single imaging mode, the pellicle has to be removed from the optical path and the mirror M1 must be replaced with a beam splitter.

To show the utility of using MPCI to study the shock response of materials, the results for two similar experiments are shown: one that used the traditional velocimetry diagnostics to measure the shock velocity and another that used the MPCI system to measure the shock velocity *in-situ*. The traditional shock wave experiment [3, 27] is shown in Fig. 14.2 (top) and consists of a polycarbonate projectile and flyer plate impacting the polycarbonate sample. Multiple photonic Doppler velocimetry (PDV) probes [28] were positioned about the target to measure the particle velocity at the impact surface,

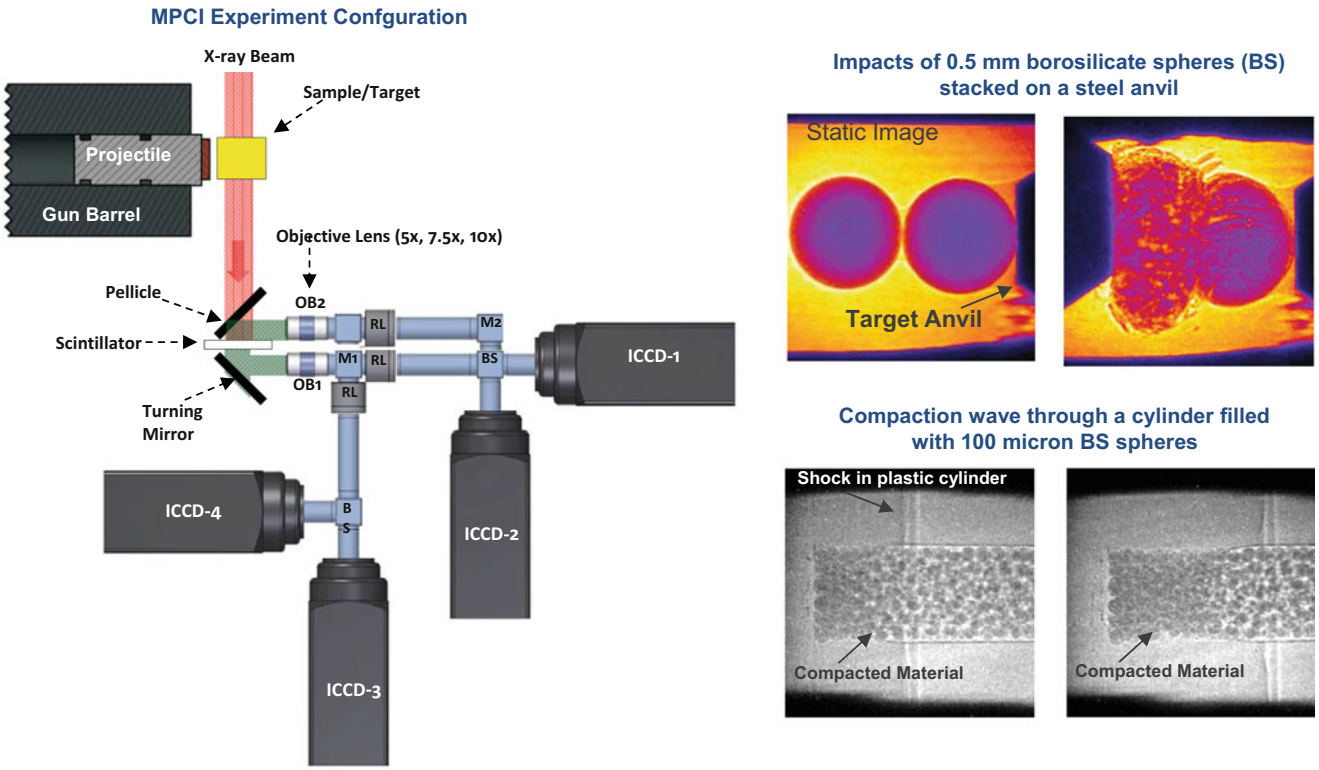

Fig. 14.1 Experiment configuration for typical X-ray PCI impact experiments using the Los Alamos Laboratory MPCI system. (Top-Right) Example PCI data showing the compaction of glass spheres [26]. Complete absorption is indicated by black and complete transmission shown as yellow (fire colormap). The data show the sphere deforming and fracturing after impact. (Bottom-right) Example of using PCI to study shock wave propagation through a tube filled with 100 micrometer borosilicate spheres to study the compaction process. The shock wave in the confining material (PMMA) is visible along with the slower moving compaction front. In both examples the shock wave or impact occurs from left to right

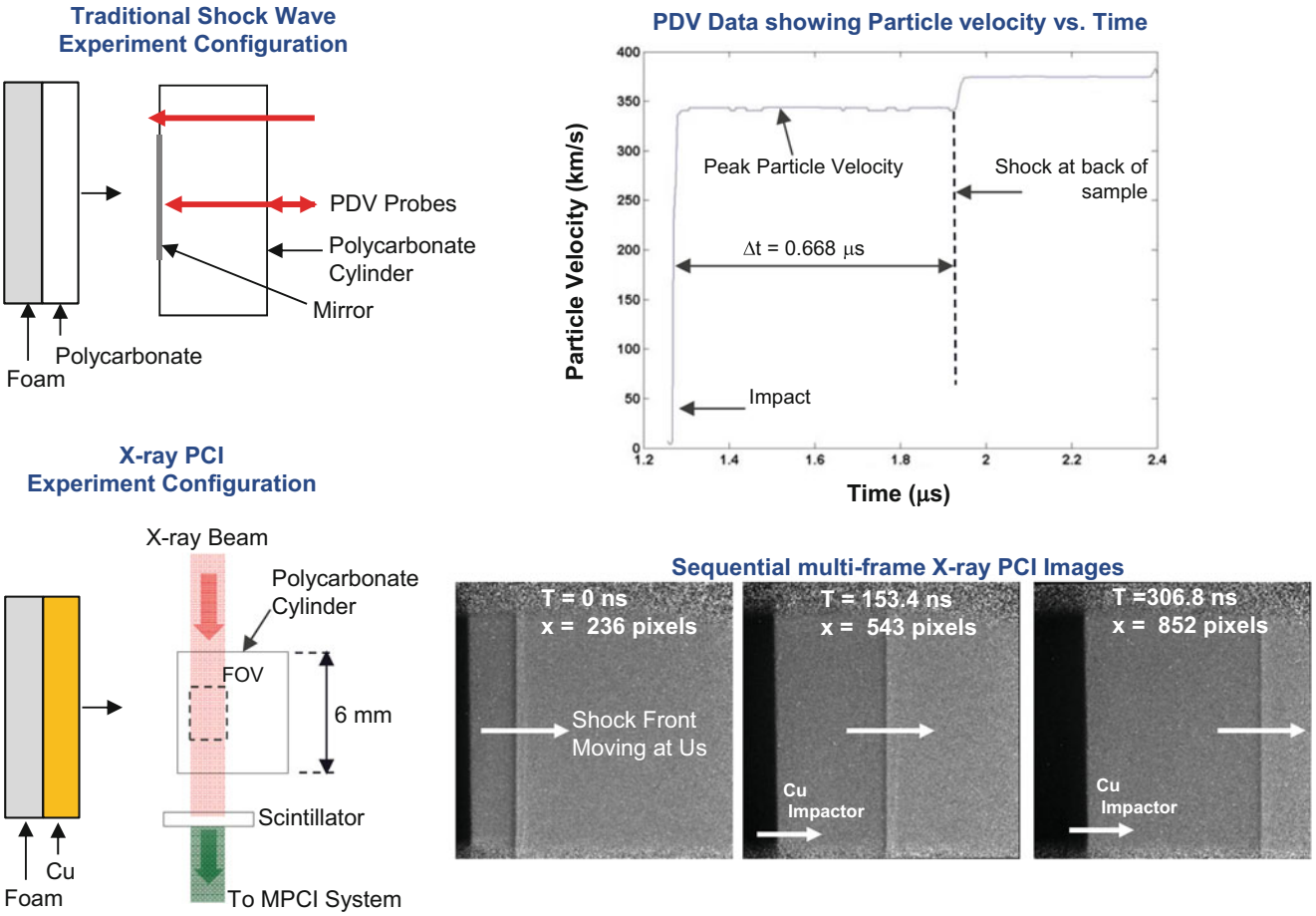

Fig. 14.2 Experiment configuration and example data for two experiments that use traditional and X-ray diagnostics. (Top) Experiment configuration for MPCI experiments along with three PCI images taken at 153.4 ns intervals to observe the shock wave propagation through polycarbonate. The shock front and copper impactor are indicated by the white arrows. The position of the shock wave in pixels is indicated by the parameter, x. (Bottom) Experiment configuration for a traditional symmetric impact (flyer and sample materials are the same) experiment to measure the particle velocity at the impact surface and the shock wave speed through the sample. Example data obtained using PDV are shown to the right. Dynamic images have been corrected using bright-field and dark-field images

back surface of the sample, and the projectile velocity up to impact simultaneously. Because the polycarbonate samples are transparent to the 1550 nm laser light used in the PDV, the shock wave speed can be measured directly using a single PDV probe located on the center of the sample. In contrast, the experimental configuration for the X-ray PCI experiments performed on the IMPULSE gas gun system at Sector 35 of the APS is shown in Fig. 14.2 (bottom). A polycarbonate projectile fitted with a copper flyer plate impacted a polycarbonate cylinder (sample) generating a steady shock wave the propagated through the material. X-rays were transmitted through the sample and were detected using the MPCI system to obtain images of the shock wave as a function of time. For all experiments, multiple images were taken including dark-field images to measure the camera background with no X-rays and bright-field images (X-ray beam with no sample) to calibrate 100% transmission, variations in the X-ray beam itself, and to account for phase contrast features along the beam line (e.g. dust, imperfections in window materials, etc.). Static images (pre-shot) were taken to position the object and visualize features prior to the experiment. A detailed description of the PCI analysis can be found elsewhere [26].

14.3 Results

Example data for the traditional, symmetric impact experiment is shown in Fig. 14.2 (top) [27]. The measured projectile velocity was Vp = 0.674 ± 0.001 km/s. The PDV data is shown in Fig. 14.2 (top-right) where the particle velocity (km/s) is plotted versus time (μs). A velocity jump to a steady state particle velocity of $u_p = 0.343 \pm 0.005$ km/s was observed at t = 1.27 μs. This steady state persists in the PDV data until the shock wave reaches the back surface of the sample at

t = 1.938 μs resulting in a release wave that propagates back through the sample. The difference between the shock jump and the shock arrival at the back surface is the transit time for the shock wave determined to be Δt = 0.668 μs. Given the known thickness of the polycarbonate sample (1.919 mm), the shock velocity was determined to be 2.873 ± 0.005 km/s in reasonable agreement with the calculated value of Us = 2.838 km/s obtained from the available Hugoniot data [29–31].

Example data obtained using the MPCI are shown in Fig. 14.2 (bottom-right) as three images taken 153.4 nanoseconds apart. The typical FOV was approximately 1.4 mm square (7.5× objective) with a pixel size of 1.687 μm/pix. The data show a well-defined shock front propagating through the sample from the left to the right (in successive images), and indicated by the white arrow that shows the direction of propagation. The copper flyer appears as the black region (100% X-ray absorption) coming into the FOV on the left of each image. The measured projectile velocity was Vp = 0.717 ± 0.001 km/s. To determine the shock wave velocity, horizontal lineouts were obtained from the images and averaged together to locate the position of the shock front at each time step. These are shown in the images as x = 236, 543, and 852 pixels (± 5 pixels uncertainty in locating the shock front) for X-ray bunch times of t = 0, 153.4, and 306.8 nanoseconds, respectively. The shock wave positions were plotted versus time and then fit to a line with the slope equal to the shock wave velocity. The resulting shock velocity was Us = 3.388 ± 0.055 km/s in reasonable agreement with the calculated value of Us = 3.323 km/s obtained from available Hugoniot data [29–31].

14.4 Conclusions

Recent developments in coupling dynamic loading platforms to the X-ray beam lines at the APS are providing new methods for diagnosing shock physics experiments. In this work, two experiments were performed that used a traditional shock method to measure shock velocity and compared it to a similar experiment that used X-ray PCI to measure the shock wave velocity directly as it propagated through the material. Overall, the two methods resulted in shock wave speeds that are in reasonable agreement with predicted values. The traditional, optical technique does result in lower uncertainty in the shock velocity measurement, however it is a useful method only for materials that are optically transparent. The MPCI method will be essential for situations where the materials are opaque, when the shock wave profile exhibits a complex structure, and/or when the materials themselves are heterogeneous (e.g. additively manufactured materials, granular systems, powders, etc.). Efforts are underway to use the PCI images shown here to calculate the density behind the shock front to better characterize the high-pressure state of the material. The ability to measure shocked density states will pave the way for the analysis and understanding of more complicated materials such as powders, granular systems, foams, and other engineered materials.

Acknowledgements This work was performed by Los Alamos National Laboratory (LANL) at Los Alamos and at the Dynamic Compression Sector (DCS) at the Advanced Photon Source (APS). All x-ray phase contrast images shown here were obtained using LANL's multi-frame x-ray phase contrast imaging system (MPCI) developed on the IMPULSE capability at APS. Chuck Owens, Joe Rivera, and John Wright (LANL) are thanked for sample assembly, experiment preparation and execution. Nick Sinclair and Adam Schuman (DCS/WSU) are thanked for their technical support at the Sector 35 beamline setting up the X-ray beam. The authors gratefully acknowledge the financial support provided by Science Campaigns, Joint Munitions Program (JMP), and National Security Technologies (NSTec) Shock Wave Physics Related Diagnostic (SWRD) program. LANL is operated by Los Alamos National Security, LLC for the U.S. Department of Energy (DOE) under Contract No. DE-AC52-06NA25396. DCS is supported by the Department of Energy (DOE), National Nuclear Security Administration, under Award Number DE-NA0002442 and operated by Washington State University (WSU). This research used resources of APS, a U.S. Department of Energy (DOE) Office of Science User Facility operated for the DOE Office of Science by Argonne National Laboratory under Contract No. DE-AC02-06CH11357.

References

1. Asay, J.R., Fowles, G.R., Duvall, D.E., Miles, M.H., Tinder, R.F.: Effects of point defects on elastic precursor decay in LiF. J. Appl. Phys. **43**, 2132 (1972)
2. Dolan, D.H., Johnson, J.N., Gupta, Y.M.: Nanonsecond freezing of water under multiple shock wave compression: continuum modeling and wave profile measurements. J. Chem. Phys. **123**, 064702 (2005)
3. Jensen, B.J., Gray, G.T., Hixson, R.S.: Direct measurement of the α-ε transition stress and kinetics for shocked iron. J. Appl. Phys. **105**, 013502 (2009)
4. Jensen, B.J., Cherne, F.J.: Dynamic compression of cerium in the low-pressure γ-α region of the phase diagram. J. Appl. Phys. **112**, 013515 (2012)
5. Jensen, B.J., Gupta, Y.M.: Time-resolved x-ray diffraction experiments to examine the elastic-plastic transition in shocked magnesium-doped LiF. J. Appl. Phys. **104**, 013510 (2008)

6. Jensen, B.J., Gupta, Y.M.: X-ray diffraction measurements in shock compressed magnesium doped LiF crystals. J. Appl. Phys. **100**(5), 053512 (2006)
7. Kalantar, D.H., Belak, J.F., Collins, G.W., Colvin, J.D., Davies, H.M., et al.: Direct observation of the $\alpha-\epsilon$ transition in shock-compressed iron via nanosecond X-ray diffraction. Phys. Rev. Lett. **95**, 075502 (2005)
8. Jensen, B.J., Lou, S.N., Hooks, D.E., Fezzaa, K., Ramos, K.J., Yeager, J.D., Kwiatkowski, K., Shimada, T., Dattelbaum, D.M.: Ultrafast, high resolution, phase contrast imaging of impact response with synchrotron radiation. AIP Adv. **2**(1), 012170–012176 (2012)
9. Luo, S.N., Jensen, B.J., Hooks, D.E., Fezzaa, K., Ramos, K.J., Yeager, J.D., Kwiatkowski, K., Shimada, T.: Gas gun shock experiments with single-pulse x-ray phase contrast imaging and diffraction at the advanced photon source. Rev. Sci. Instrum. **83**(7), 073903 (2012)
10. Jensen, B.J., Owens, C.T., Ramos, K.J., Yeager, J.D., Saavedra, R.A., Iverson, A.J., Luo, S.N., Fezzaa, K.: Hooks DE impact system for ultrafast synchrotron experiments. Rev. Sci. Instrum. **84**(1), 013904–013905 (2013)
11. Gupta, Y.M., Turneaure, S.J., Perkins, K., Zimmerman, K., Arganbright, N., Shen, G., Chow, P.: Real-time, high-resolution x-ray diffraction measurements on shocked crystals at a synchrotron facility. Rev. Sci. Instrum. **83**(12), 123905 (2012)
12. Montgomery, D.S., Nobile, A., Walsh, P.J.: Characterization of National Ignitition Facility cryogenic beryllium capsules using x-ray phase contrast imaging. Rev. Sci. Instrum. **75**, 3986–3988 (2004)
13. Yeager, J.D., Luo, S.N., Jensen, B.J., Fezzaa, K., Montgomery, D.S., Hooks, D.E.: High-speed synchrotron X-ray phase contrast imaging for analysis of low-Z composite microstructure. Compos. A: Appl. Sci. Manuf. **43**(6), 885–892 (2013). https://doi.org/10.1016/j.compositesa.2012.01.013
14. Ramos, K.J., Jensen, B.J., Yeager, J.D., Bolme, C.A., Iverson, A.J., Carlson, C.A., Fezzaa, K.: Investigation of dynamic material cracking with in situ synchrotron-based measurements. In: Song, B., Casem, D., Kimberley, J. (eds.) Dynamic Behavior of Materials, vol. 1, pp. 413–420. Springer International Publishing, Dordrecht (2014). ISBN 978–3–319-00770-0
15. Jensen, B.J., Cherne, F.J., Ramos, K.J., Iverson, A.J., Carlson, C.A., Yeager, J.D., Fezzaa, K., Dimonte, G., Hooks, D.E.: Multiphase material strength determined through shock generated Richtmyer-Meshkov instabilities. J. Appl. Phys. **118**, 195903 (2015)
16. Brown, E.N., Ramos, K.J., Dattelbaum, D.M., Jensen, B.J., Gray III, G.T., Matterson, B.M., Trujillo, C.P., Martinez, D.T., Pierce, T.H., Iverson, A.J., Carlson, C.A., Fezzaa, K., Furmanski, J.: In situ and postmortem measures of damage in polymers at high strain-rate. Conference Proceedings of the Society for Experimental Mechanics Series. **65**(1), 53–59 (2015)
17. Brown, E.N., Furmanski, J., Ramos, K.J., Dattelbaum, D.M., Jensen, B.J., Iverson, A.J., Carlson, C.A., Fezzaa, K., Trujillo, C.P., Martinez, D.T., Gray III, G.T., Patterson, B.M.: High-density polyethylene damage at extreme tensile conditions. J. Phys. Conf. Ser. **500**, 112011 (2014)
18. Hawreliak, J., Lind, J., Maddox, B., Barham, M., Messner, M., Barton, N., Jensen, B.J., Kumar, M.: Dynamic behavior of engineered lattice materials. Nature Scientific Reports. **6**, 28094 (2016)
19. Branch, B., Ionita, A., Clements, B., Montgomery, D., Jensen, B.J., Patterson, B., Mueller, A., Dattelbaum, D.M.: Controlling shockwave dynamics using architecture in periodic porous materials. J. Appl. Phys. **121**, 135102 (2017)
20. Willey, T.M., Champley, K., Hodgin, R., Lauderbach, L., Bagge-Hansen, M., May, C., Sanchez, N.J., Jensen, B.J., Iverson, A.J., Van Buuren, T.: X-ray Imaging and 3D Reconstruction of In-Flight Exploding Foil Initiator Flyers. J. Appl. Phys. **119**, 235901 (2016)
21. Sanchez, N.J., Neal, W.E., Jensen, B.J., Iverson, A.J., Carlson, C.A.: Dynamic Exploding Foil Initiator Imaging at the Advanced Photon Source. AIP Conf. Proc. **1979**(160023), (2018)
22. Neal, W.E., Sanchez, N., Jensen, B.J., Gibson, J., Martinez, M., et al.: The effect of surface heterogeneity in exploding metal foils. AIP Conf. Proc. **1979**(180007), (2018)
23. Mandal, A., Jensen, B.J., Aslam, T.D., Iverson, A.J.: Dynamic Compaction of Nickel Powder Examined by X-ray phase contrast imaging. AIP Conf. Proc. **1979**(110010), (2018)
24. Ramos, K.J., Jensen, B.J., Hooks, D.E., Fezzaa, K., Yeager, J.D., Iverson, A.J., Carlson, C.A., Cherne, F.J.: In situ investigation of the dynamic response of energetic materials using IMPULSE at the advanced photon source. J. Phys. Conf. Ser. **500**, 142028 (2014)
25. Jensen, B.J., Hooks, D.E., Fezzaa, K., Ramos, K.J., Yeager, J.D., Iverson, A.J., Carlson, C.A., Cherne, F.J., Kwiatkowski, K.: Dynamic experiments using IMPULSE at the advanced photon source. J. Phys. Conf. Ser. **500**, 042001 (2014)
26. Jensen, B.J., Montgomery, D.S., Iverson, A.J., Carlson, C.A., Clements, B., Short, M., Fredenburg, D.A.: X-ray phase contrast imaging of granular systems. LA-UR-17-27104 Los Alamos Laboratory Report (2017)
27. Branch, B., Jensen, B.J.: Dynamic X-ray diffraction to study the shock-induced a-e phase transition in iron. AIP Conf. Proc. **1979**(040001), (2018)
28. Jensen, B.J., Holtkamp, D.B., Rigg, P.A., Dolan, D.H.: Accuracy limits and window corrections for Photon Doppler velocimetry. J. Appl. Phys. **101**, 013523 (2007)
29. *LASL SHOCK HUGONIOT DATA* (University of California Press, Berkley and Los Angeles, CA, 1980)
30. Carter WJ, Marsh SP. Hugoniot Equation of State of Polymers. LA-12006-MS Los Alamos National Laboratory (1995)
31. Millett, J.C.F., Bourne, N.K.: Shock and release of polycarbonate under one-dimensional strain. J. Mater. Sci. **41**, 1683–1690 (2006)